Wireless Joint Motion Tracking

Stephen Mock
Adaptive Robotic Manipulation Lab
Georgia Institute of Technology
Atlanta, United States
smock6@gatech.edu

***Abstract* — This paper describes my second semester working on developing and testing the technologies of wireless joint motion tracking units. The goal of the project is to design repeatable, accurate, and low form factor units to measure positions of serially linked manipulators. The technology can be applied to augment robotic devices with position and angle sensing, especially where the range and accuracy of traditional joint tracking is inadequate. These units house a magnetic hall effect sensor to read angle position and a wireless communication system. Using forward kinematics, the angles read by the sensor can be turned into positions. In order to test the accuracy of the hall effect sensors, a 1 degree-of-freedom (DOF) test rig was developed. The test rig implements PI (proportional–integral) control, motor control, and encoders, to obtain a ground truth angle measurement. This measurement is later compared with the sensor's measurements to evaluate accuracy.**

***Keywords* — serial communication, I2C (inter-integrated circuit), SPI (Serial Peripheral Interface), motor control, PID, microcontroller, State Machine**

I. Introduction

This paper documents my progress during the Spring 2020 Semester working as an undergraduate within Dr. Hammond's Adaptive Robotic Manipulation Lab. Bryan Blaise, my graduate mentor from the Department of Mechanical Engineering at Georgia Institute of Technology, developed the initial project idea, and helped direct my work throughout the semester. This is my second semester working on this project.

Joint position sensing is necessary for most robotic systems. Traditionally, joint position sensing is accomplished through encoders, rotary sensors, or other methods such as computer vision tracking [1]. Position can also be derived from accelerometer kinematic data. However, many of these methods are often costly, unreliable, and tethered which limits robot/user workspaces.

Magnetic hall effect sensors can be used to measure rotational angle in many common components such as motors, wheels, and valves [2]. By using hall effect sensors to measure joint position, a cheaper and lower form factor alternative is possible when compared to traditional sensing methods. Coupled with wireless tracking that is scaled for robotic devices, these units are easy to implement when determining joint angles.

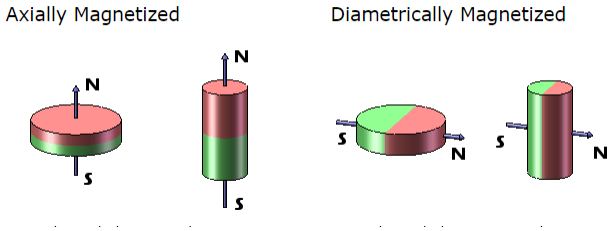

Figure 1. Direction of magnetic field for Axial vs. Diametric magnets.

To understand the application of the hall effect sensor, the characterization of magnets must first be discussed. For hall effect sensor applications, magnets are generally either axially, or diametrically magnetized [3]. Depending on the magnetization, the plane in which the magnetic field lies in differs. For the primary application of 3D sensing hall sensors, diametric magnets are often preferred.

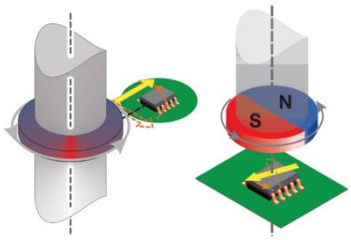

Figure 2. Various orientations of hall effect sensors. Left: Off Axis Right: On Axis

Regarding hall effect sensors, they also have various orientations. The orientations are either off axis, or on axis. On axis is the preferred method of sensing, as it is more accurate and has less variation in magnet field sensing [4]. Off axis sensing has a wide variation in magnetic field, and often requires digital post processing of raw measurements to get an accurate output. Common techniques of post processing include Harmonic linearization.

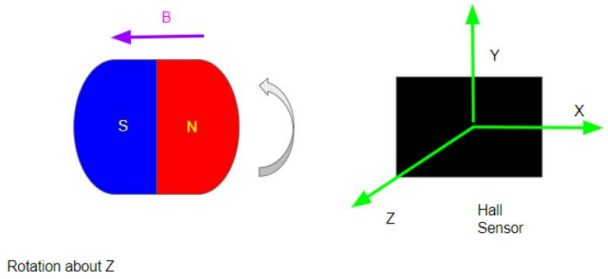

Figure 3. Initial position and orientation of off axis magnet and hall sensor.

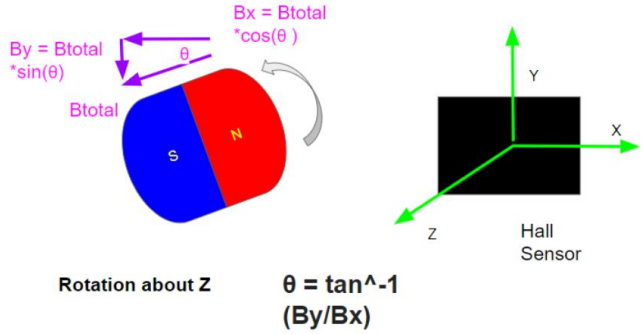

Figure 4. Calculation of angle regarding the rotation of magnet.

The hall sensor is able to measure the strength of magnetic fields in X, Y and Z axes in the unit of Guass. Using this information, it is possible to calculate the measured magnetic angle with some basic trigonometry as seen in Fig. 3, Fig 4 and Equation (1). With the angle of the magnet being known, forward kinematics can be applied to calculate joint position, assuming rigid links. For these applications, an off-axis orientation will most likely be used. The magnet will be attached to one link of the joint, and the sensor will be stationary nearby. This will allow for determining the relative rotation between the two as the magnet moves.

$$\Theta = \tan^{-1}(B_y / B_x) \quad (1)$$

In order to begin development of the units, a 1DOF test rig was constructed to test the validity of the hall effect sensors. The test rig incorporates a motor and coupler with an attached magnet and uses an Arduino microcontroller for processing. Using PI control, encoders, and motor control, the angular position of the motor shaft can be accurately determined. This way the shaft position can act as a ground truth, when compared to the angle measured by the hall effect sensor.

Overall design considerations for the project included effective sampling speed for wireless communications, accuracy of magnetic sensors, size of system, and magnetic effect on sensors due to proximity of one another. The rest of this report details the process, construction and results of designing the test rig and code.

II. METHODS

A. *Libraries*

With the help of online sources [5], I wrote my own custom I2C and SPI libraries to make my code more modular. This helped to make the already high-level Arduino code even more encapsulated in a way I could easily implement. Additionally, I documented the libraries so that they could be used by future students in the lab. Figure 5 and 6 list the various methods and their functionalities.

Function Name	Functionality
readI2C	Reads specific device address and register; read one byte
readMultiI2C	Reads specific device address and register, writes an array of bytes to register
writeMultiI2C	Writes a specific number of bytes to a specific device and register; returns if the operation was successful

Figure 5. I2C library functions and their uses.

Function Name	Functionality
writeSPI	Write one byte
writeMultiSPI	Writing an array of bytes
writeThenReadSPI	Write a number of bytes, then read a number of bytes
readSPI	Read one byte from a register
writeAndReadSPI	Write a byte, then read a byte; done multiple times

Figure 6. SPI library functions and their uses.

B. *Design and Fabrication of Test Rig*

The test rig can be split into four main components: the mechanical system, encoder and quadrature counter, motor driver, and the magnetic hall effect sensor. The following sections will explain each in more detail.

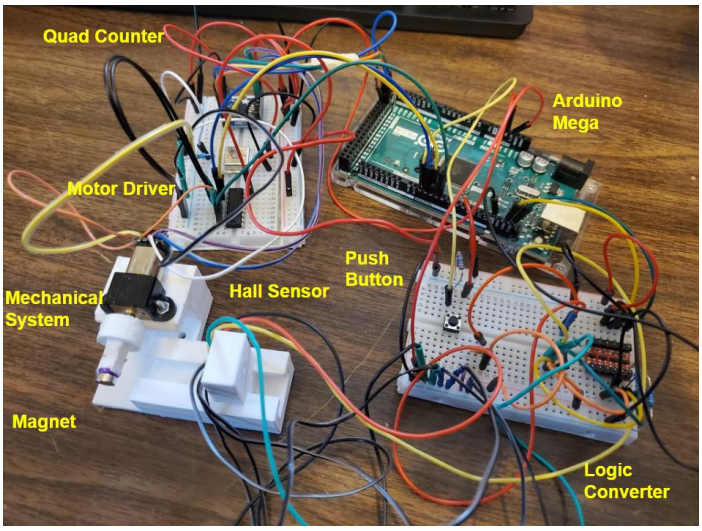

Figure 7. 1DOF Test Rig and its subcomponents.

a) Mechanical System: The mechanical system consists of 6 components: the motor, motor brace, the motor coupler, magnet, magnetic sensor mount, and the base itself. The system was originally designed on SolidWorks, and then various iterations were 3D printed. The motor coupler is attached to the motor's flat side of the shaft using a set screw and nuts. On the motor coupler end, a diametric disc magnet sits flush. The motor is attached to the base of the system using a motor brace, screws, and nuts. The hall effect sensor is able to be press fit into the magnetic sensor mount. Additionally, the height of the magnet is aligned with that of the magnetic sensor. For the system to work, the motor rotates the magnet to a specific angle, and the magnetic sensor is able to calculate the perceived angle from the magnet. In order to test how the sensor accuracy varies with 1DOF, the magnetic sensor mount is able to slide away from the magnet. From last semester, the orientation and placement of the magnet has changed, as it was originally incorrect. Additionally, the motor brace orientation was slightly adjusted in order to allow for all of the components to fit flush, as this was an issue last semester. Because the sensor being used is also different, a new magnetic sensor mount design was created and tested so that the sensor fits well.

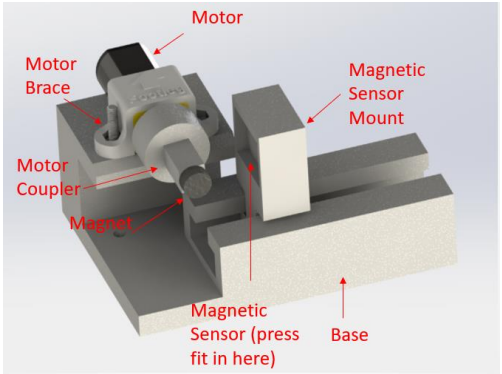

Figure 8. Mechanical System and its subcomponents (CAD)

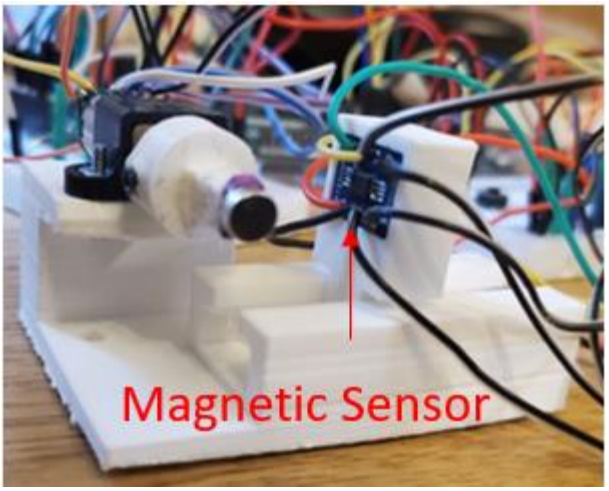

Figure 9. Close up of real test rig containing magnetic sensor in mount.

b) Magnetic Sensor:

Figure 10. ALS31313 Hall Sensor.

The sensor that was selected was the ALS31313 [6]. It was chosen because it had thorough documentation and example code. Additionally, the sensor has a range of ±2000 Gauss, runs with a sampling rate of 3KHz, and uses I2C. Regarding the range required, the magnet that is used (Radial Magnet #8995), has a strength of 3873 surface Gauss [7]. Because Magnet strength has a rough correlation of $F \propto (1/r^2)$, where r is in units of cm, it seems to relatively fit the magnitude that the sensor can measure. This is particularly useful information as the distance of the sensor to the magnet can be adjusted in 1 DOF. Some nuance is that the sensor model that was purchased is ALS31313KLEATR-2000, which has a range of ±2000 Gauss, and a sensitivity of 1LSB/Gauss. This is different from other models which have a lower range, which is less useful in a moving environment where measurement magnitudes vary greatly.

Figure 11. Radial Magnet #8995, Diametric Magnet.

Additionally, because the Arduino communicates with 5V logic, a 5V to 3.3V logic converter was used [8].

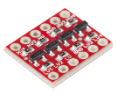

Figure 12. 5V to 3.3V Logic Level Converter.

Source code was then written to measure the angle in accordance with Fig. 4 and Equation (1). With this value from the sensor, the angle can be compared with the ground truth value from the encoder. The code behind the sensor will be explained in further sections.

c) Encoder and Quadrature Counter: The motor that was used in the mechanical system was a Pololu 12V Micro Motor [9]. Attached to the back of the motor is a magnetic quadrature encoder. The encoder allows for accurate measurement of shaft rotation. The shaft on the front and back of the motor had a gear ratio of 1:29.86, which provides about a 1-degree resolution. This was taken account of when calculating the value of angular rotation for the main shaft.

Figure 13. 12 Volt Micro Motor and Encoder.

In order to prevent timing issues when calculating the encoder angle, a LS7336R quadrature counter was used [10]. Along with the LS7336R, a MX045HS oscillator was used to set the counter's clock frequency [11]. Source code was then written using the SPI library I had created, and the encoder system was tested.

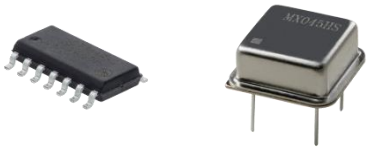

Figure 14. LS7336R Quadrature Counter (left), MX045HS Oscillator (right).

d) Motor Driver: The final component was to implement a motor driver to accurately control the motor. To do this, a L293D motor driver was used [12]. PWM (Pulse Width Modulation) was used to control the speed of the motor. Because the L293D has H-Bridges, the direction that the motor rotated could also be controlled. This was important to implement so that the motor can be precisely turned to a specific degree. Specific motor functions for speed and direction control were written in order to make coding more modular. Issues arose due to voltage draw when using batteries to power the motor, so a power supply had to be used. For testing, I ran the motors at a maximum of 9V.

Figure 15. L293D Motor Driver.

A full electrical diagram with many of the various components is shown below:

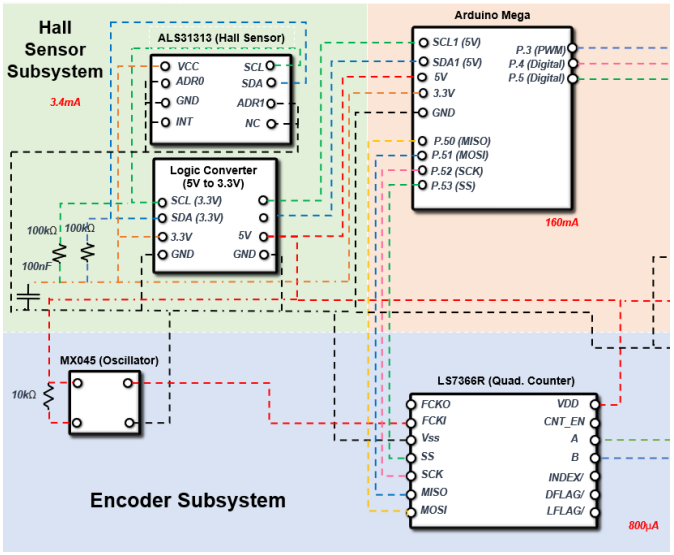

Figure 16. Wiring Diagram for Hall Sensor, Quad Counter, and Arduino.

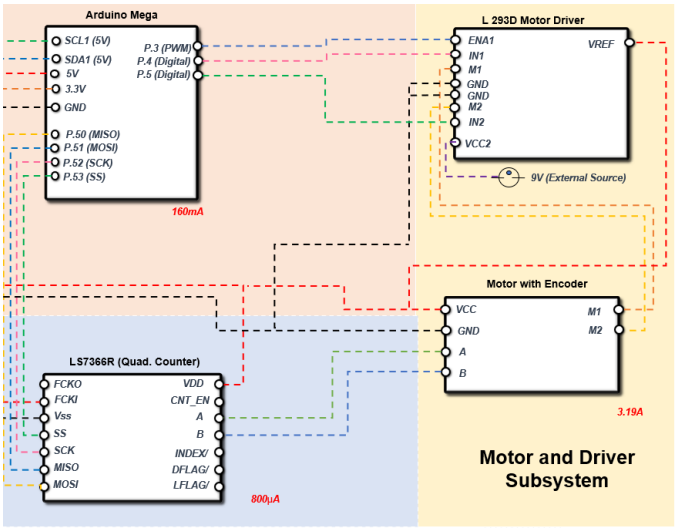

Figure 17. Wiring Diagram for Motor Driver and Motor, with Quad Counter and Arduino

C. 1DOF Test Rig PID Control

In order to begin testing the accuracy of the magnetic sensor, first the motor needed to reliably reach angles. The four main components were combined into one system. Using PID control, the angle values recorded by the encoder could be used to account for error and ensure an amount of motor rotation.. For my PID system, I used Proportional and Integral control to start. Integral control was very important as it helped to reduce steady state error due to motor stalling at low voltages.

Dampening was not used because the system did not move quickly enough to justify adding more complexity and tuning. Below, Fig. 18 demonstrates the system's block diagram.

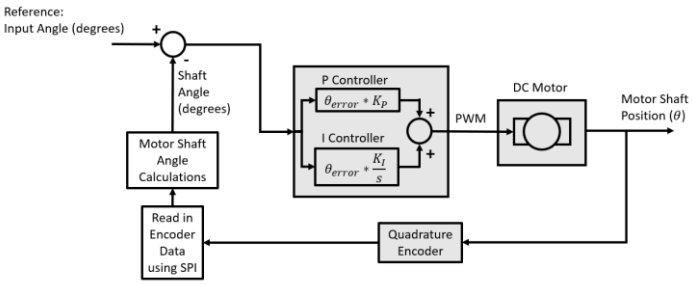

Figure 18. Test Rig Control Block Diagram.

The system starts with a reference angle, and the error between the real measured angle is calculated. This error is multiplied by a proportional gain constant, Kp, and the value is an input to the microcontroller. Within the code, this error is mapped to a voltage between -9V to 9V, where the negative denotes the rotation direction. 9V corresponds to 255 in my code, which is the max duty cycle in terms of PWM that can output to the motor driver. This value is then used to control the speed and direction of the motor. The goal is to then tune Kp and Ki so that the system is stable, and the desired angle is achieved. At this point, magnetic measurements can be acquired, and compared to that of the encoder.

D. Code

In order to best test the validity of the hall effect sensor, various encoder values needed to be compared to the angle calculated by the hall sensor. To do this, the motor must rotate to a specific angle, then the hall sensor obtains measurements at this location. Because my system is using multiple sensors, timers, and PI Control, a state machine was used. This state machine helped to control the flow of the code. The program also uses two Arduino timer libraries, Timer1 and MsTimer2.

For the test rig code, the state machine uses a push button to cycle between states. The state machine works by initially polling at a "resting state" where no measurements occur. The next state is where the PI control takes place, rotating the motor to a specific angle. The third state then waits for a button press to begin hall effect sensor measurements. The fourth state is when magnet data is measured and can be copied from the serial monitor (or potentially UART if implemented). Lastly, the cycle loops back to the first state, where a new angle can be rotated to. A diagram of the state machine is shown:

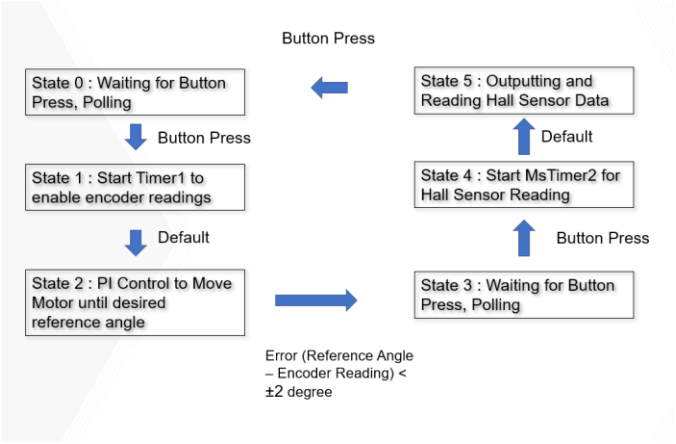

Figure 19. State Machine diagram with transitions.

The ASL31313 sensor worked by storing raw magnet data in two 32-bit registers. These registers are 0x28 and 0x29. Regarding the actual measurements, data was presented in 12 bits, eight from 0x28, and 4 from 0x29. Both registers needed to be concatenated for meaningful data. Additionally, prior to any measurements a customer access code must be entered at address 0x35, with data 0x2C413534. The sensor also has various settings, Single Mode, Fast Loop Mode, and Full Loop mode [13]. Each have their own benefits and varying complexity, but Single Mode was used for simplicity. Additional testing could be performed to test performance using different settings.

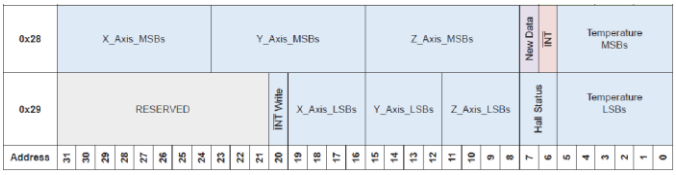

Figure 20. Important registers for the ALS31313 sensor. Each register is 32 bit, where data is represented in 12 bits.

The code has three main functions, readALS31313, readCount, and PIControl. The following section will explain each briefly.

a) readALS31313

This function takes in inputs of a float array and device address for I2C. This function uses another sub-function which utilizes my I2C library, I2CreadRegister32bit. This sub function saves the data from the 32 bit registers, in a length 4 array which holds 8 bit data. readALS31313 then combines the respective registers for X,Y,Z magnet data into their twelve bit representation. Then, the function converts the raw data into angle measurements, and stores it into the inputted floating array.

b) readCount

This function utilizes my SPI library, and stores 32 bit register data from the quadrature encoder into an array of length 4, with 8 bit data. The return value is a long, which represents the number of ticks that the encoder has measured. Using the

tick count, shaft position can be determined by dividing by the resolution (1° for my motor).

c) PIControl

This function takes a reference angle, and current encoder reading, and passes these values into a sub-function controlUpdate. controlUpdate calculates the respective error using a PI controller and returns this value. PIControl, then maps a corresponding PWM (0-255 corresponding to 0–9V) based on the error, and this value controls the speed of the motor. The sign of the error also determines the rotation direction.

Using the now developed mechanical system, control algorithm and code, various tests were conducted.

III. RESULTS AND DISCUSSION

The following section outlines results found during testing of the system and sensor.

a) Mechanical Design: Last semester, issues arose regarding mounting the motor upon the test rig base and wire spacing from the encoder. This is shown in Figure 21.

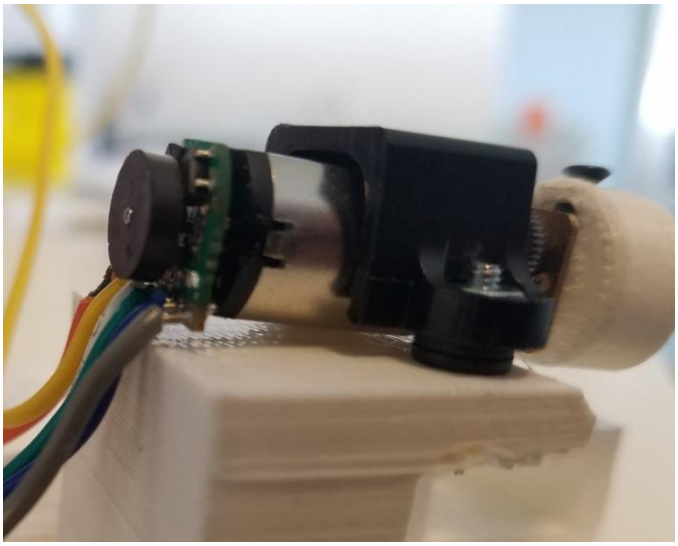

Figure 21. Mechanical issues present in previous assembly.

By slightly adjusting the positioning of the motor brace, the motor was able to be succesfully mounted flush on the base without washers. However, the motor coupler needed to be moved slightly forward, which slightly unalligns it with the sensor. Additionally, smaller and more flexible wires were attached to the encoder, and the orientation of the encoder was flipped, allowing for better spacing. The changes are shown in Figure 22.

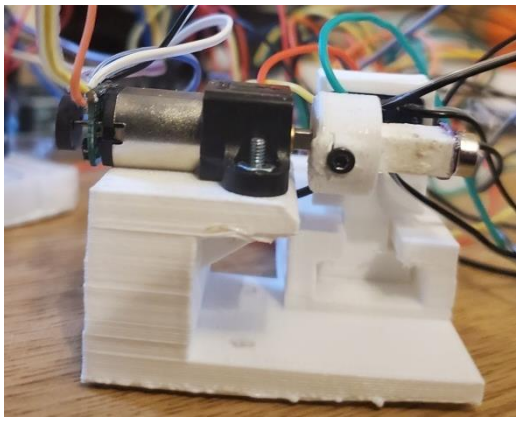

Figure 22. Current assembly of mechanical system. There is no interference with the motor brace and encoder unlike before.

During the semester, I realized that my understanding of the physical interpretation of the sensor and magnetic field orientation was incorrect. Previously, I had planned to place a magnetic sheet on the shaft of the motor coupler, however that would not result in the angle of rotation I was looking for. Because I now understand how the magnet field is aligned for a diametric magnet, I still tried to use the test rig I currently had. I did this by placing the magnet on the end of the motor coupler so that the magnet would rotate about the X-axis of hall sensor, and I could find an angle in the YZ axis. This orientation is shown more clearly below.

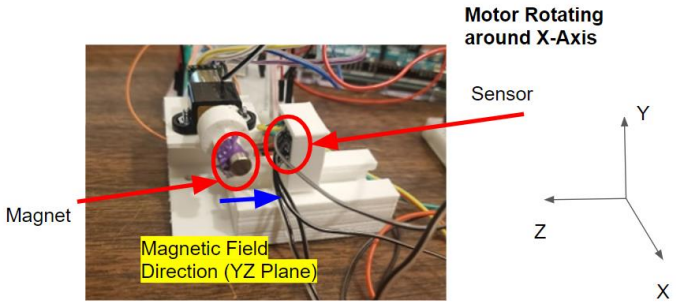

Figure 23. Test Rig orientation of both the hall sensor and magnet. The motor rotates about X axis.

Attaching the magnet to the end of the motor coupler is not an ideal setup because now, the magnet is out of line with the magnet sensor. However, the process was to still see if general trends and measurements from the sensor are usable before developing another rig. Additionally, I glued the magnet onto the coupler, as I did not have any other resources at home. A better mating mechanism is preferred.

For future development, a test rig should be designed like that shown in Figures 24 and 25. In this example, the orientation of the magnet and sensor is very clear, and the magnet simply rotates in the exact same plane.

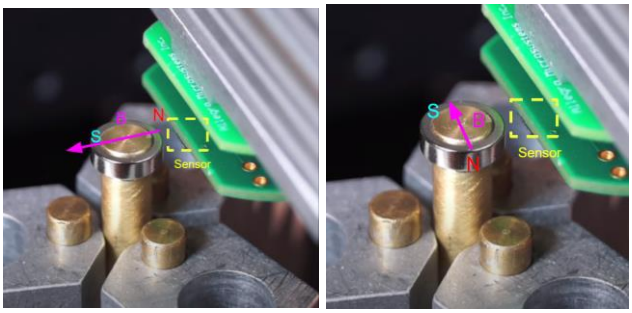

Figure 24. Preferred example test rig setup where the magnet and sensor lie in the same plane. The magnet simply rotates.

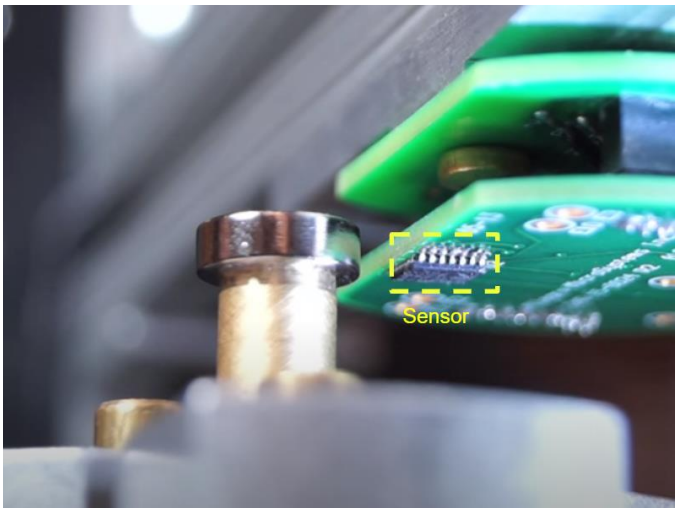

Figure 25. Another view of the example test rig.

b) Control System Redesign: Previously, the PI controller that I was using mostly worked, but had a few issues regarding timing and mapping error to PWM. Additionally, I had not been implemented Integral Control. With my current implementation, timers are now being used in order to correctly capture the error time step for integral control. Additionally, in my PI controller code, hard limits were set for how PWM is mapped so that all values stay within 0-255 (corresponding to 0-9V). Before, I had been using the Arduino map() function which has the ability to scale outside of a given bounds. During testing, the system has a fairly quick response rate, and though it still had some stalling issues at low voltages, the integral component of the error would adjust for this. Because of the resolution of the encoder (~1 degree) and the general inertia of the system, the motor was unable to reach reference angles exactly. Even with well tested proportional constants, sometimes the system would overshoot, but did not have the resolution to detect this and could only reach a certain level of precision. The controller was effective in reaching reference angles within a few degrees (in my code it is ± 2 degrees). For the purposes of my tests, the exact position of the motor in accordance to the reference does not matter, so long as within a reasonable range. The comparison of the final encoder angle to that measured by the hall sensor is what is actually important.

c) Test Results

Before any complex system can be used, the simplest form of the magnetic sensor had to be tested. To do this, a test script was written to simply test the output of the sensor, and to make sure the raw values for magnet data made sense.

First tests measured the magnet data with no magnet present and presented the following results. In the figure, blue, red and green corresponds to magnitude of magnetic field in the X,Y and Z directions respectively.

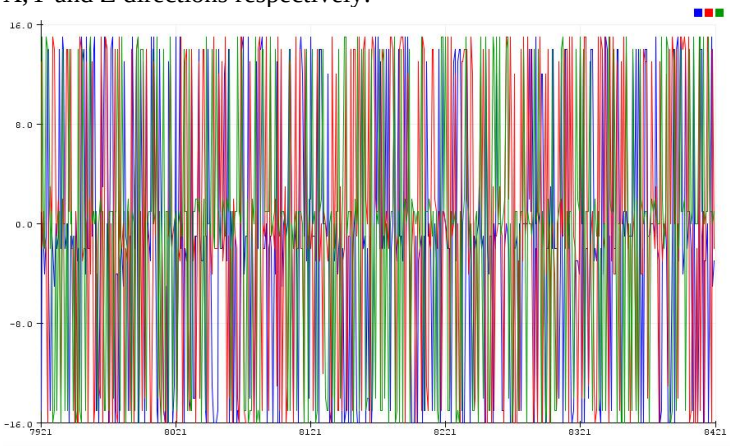

Figure 26. Magnet sensor raw output with no magnet present.

From an initial glance, there is significant noise when there is no magnet present. This could be because there is not a strong enough dominating magnetic presence, and therefore the sensor is just reading random electromagnetic interference in the room and in its wires. For all of the directions (X,Y,Z), it seems like the magnet reading noise is about the same (±16 Gauss).

When the sensor is placed closer to the magnet, the following graph is produced.

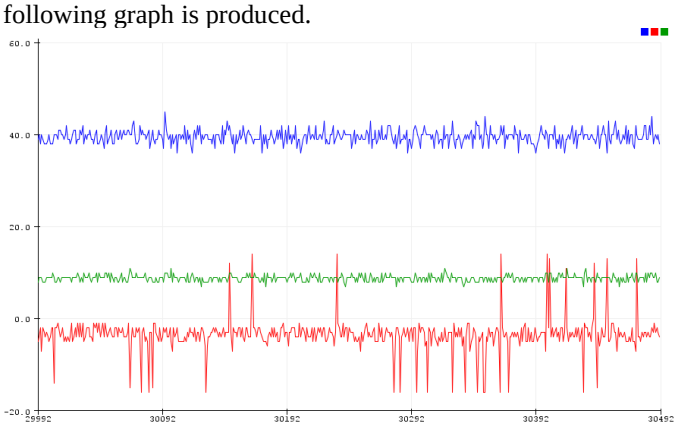

Figure 27. Magnet sensor raw output when near magnet in test rig.

Here, the relative magnitudes of the noise are much more stable, and significantly less for all three dimensions. The magnet being used however, is about 3873 Gauss; the magnitudes of the readings are quite low. When the magnet is randomly rotated, the following graph is produced.

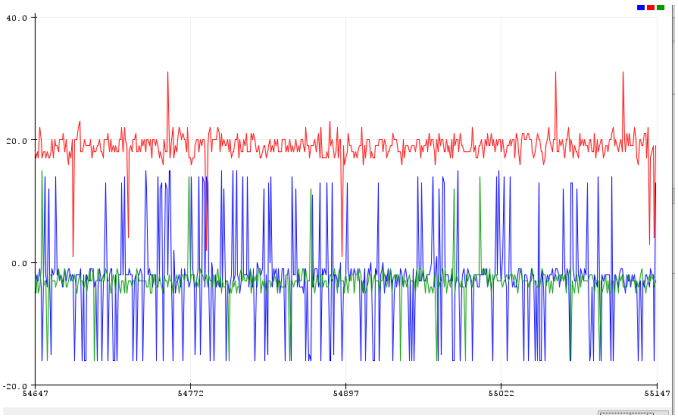

Figure 28. Magnet sensor raw output when near magnet at certain rotation.

Here, the noise of the X and Z directions is much larger. Because the magnet is in theory rotating about the X axis of the magnet, the X axis magnitude should not be changing. However, it has changed since its previous location shown in Figure 27. Based on these results, it seems like there is more noise depending on the orientation of the magnet. Because the system I have is not perfectly aligned, there can be wide variations in the magnetic field produced. Additionally, magnet fields are not just direct normalized vectors. They have curvature and have a varying strength, so it is unrealistic to represent them as one single resultant force.

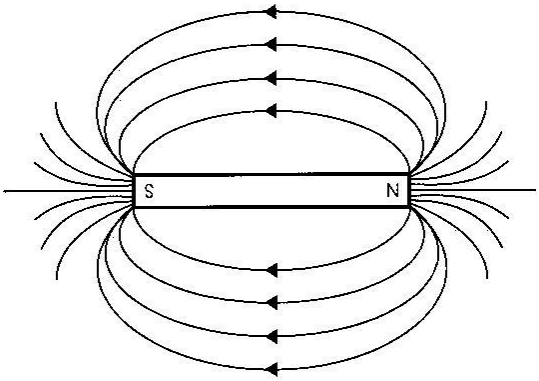

Figure 29. Example magnet field with its varying magnet fields.

To better analyze the results, basic averaging techniques were used, where a timer adds up a sum of measurements, and then averages them. For the resulting plot, 100 samples were taken every second, and then averaged:

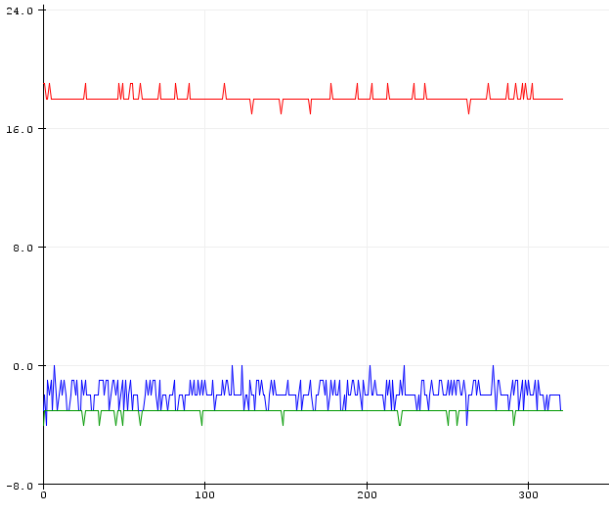

Figure 30. Magnet sensor when using filtering techniques. Averages 100 samples per second.

Here, the data looks much cleaner, and the noise is relatively small in all directions. This magnet is in the same position as that in Figure 28. Based on this, it seems like averaging signals is an effective technique when using these sensors. The noise amplitude is only about ±1 Gauss. The filtering technique was repeated and used with the sensor when there was no magnet present and the following graph was produced.

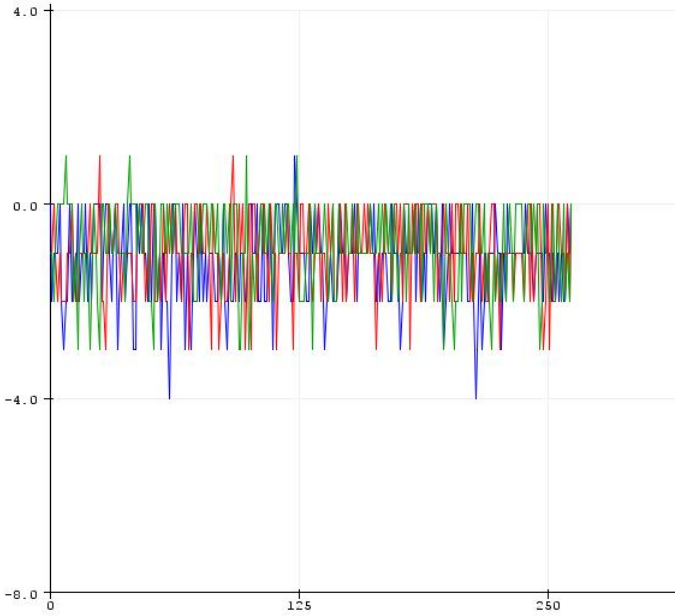

Figure 31. Magnet sensor when using filtering techniques. No magnet present.

Again, filtering is effective as the noise is significantly less than that present in Figure 26. The magnitude of this noise is about ±1 Gauss. Additionally, the values are close to zero as they should be with no magnet present. However, the effects of

the phase delay introduced by filtering should be explored in the future.

Next, using my PI controller, I rotated the magnet in 90-degree increments about every 30 seconds to see if I could observe any specific behavior. It is important to note that the exact orientation of the magnet is unknown, so 0 degrees as defined by my system is not necessarily 0 degrees of the magnet and measured by the sensor. However, relative relationships may be obtained with the change in degrees.

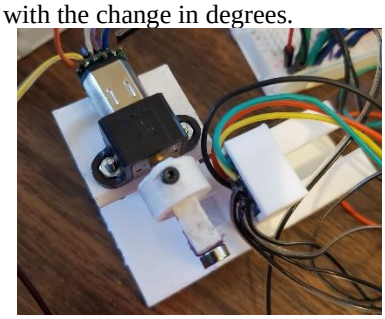

Figure 32. Orientation for tests, where the set screw being at 0 the top represents 0 degrees.

As shown, I represented 0 degrees as where the set screw is at the top.

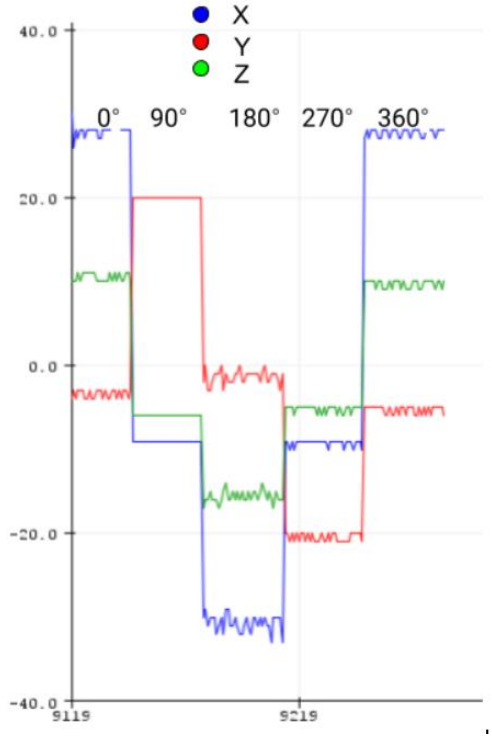

Figure 33. X,Y,Z raw magnet data (Gauss), where the magnet rotates 90 degrees clockwise every time. 0 degrees represents the set screw at the top.

From this figure, as the magnet rotates, there is noticeable change in the magnitude and sign of the magnetic field. However, it seems odd that all three dimensions are changing, as it should only be rotating around the x-axis, so that y and z should only change. The magnet magnitudes almost seem like they are following a cosine relationship. They are maximum at 0 degrees, around 0 at 90 degrees, minimum at 180 degrees, and then 0 again at 270 degrees. This makes sense because when the magnet is fully rotates, the magnet field vector should be facing the opposite direction, which seems to line up with the graph. Another figure was created by rotating at 45-degree increments. It is hard to interpret results from these graphs, but all the axes seem to follow similar trends.

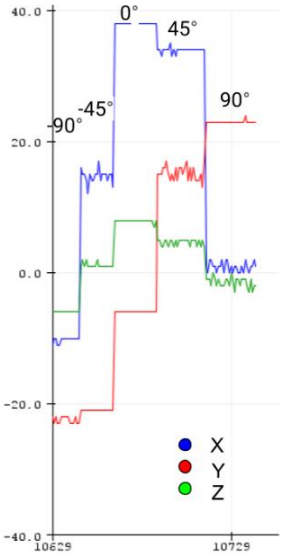

Figure 34. Repeating the process, but with 45-degree increments.

A similar analysis was performed by rotating in 90 degrees increments and then calculating the angle in the YZ plane using an analogous equation to Equation (1). The following table explores this.

Degrees of Rotation	YZ Measured (Degrees)	Absolute Change Between Measurements
0	127	134
90	-7	54
180	-61	109
270	-170	140
360	130	

Table 1. Rotating 0 to 360 degrees in 90 degree increments and recording the change in angle measurements in the YZ plane.

From this table, the change between measurements should always be ~90 degrees for each of the measurements. As seen in the last column, the changes are not 90 degrees, but in some regard, they are somewhat similar. When this test was performed in the XY and XZ planes, there was no relationship at all, so only the YZ axis was looked at as predicted. An important note is that between the 270 and 360 degree rotation, the measurement changes by about 300 degrees. However, due to the nature of the arctan function being used, the absolute difference is only 140 degrees. Based on these results, it seems like the technology has some promise as a relative relationship between magnetic angle in YZ and the encoder angle can be followed. However, without a proper test rig it is hard to make any more conclusive results. For future

tests, a more rigid test rig should be constructed and better aligned with the magnet. Because I could not print a new test rig due to restricted lab/3D printer access, it is important to note that misalignment between the sensor and magnet has significant affects.

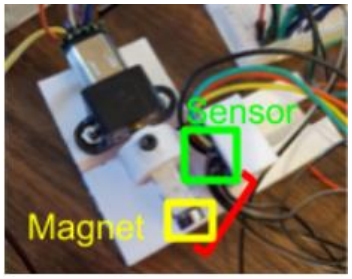

Figure 35. Large misalignment between the magnet and sensor.

A final test was conducted by placing the magnet onto a flat pen and holding the magnet on-axis over the sensor. I slowly rotated the magnet, to see what the maximum reading of the sensor could be.

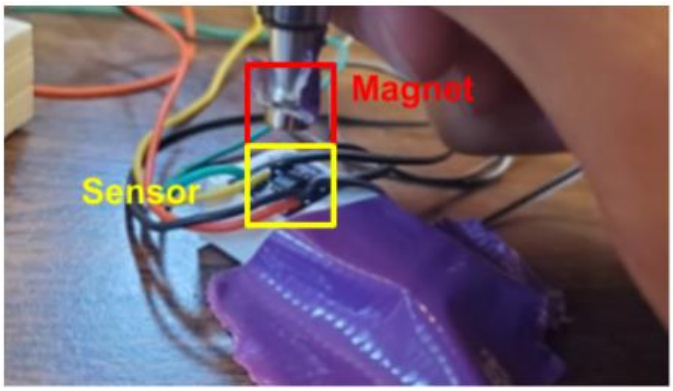

Figure 36. Setup for testing for maximum magnet reading.

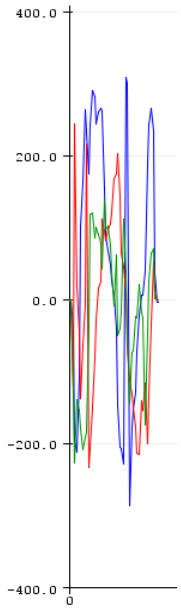

Figure 37. Testing the maximum reading of the sensor by rotating a magnet over the sensor.

This test obviously has many flaws as I could not hold the magnet stable for prolonged periods of time or exactly on axis, but it shows that the maximum Gauss that was measured by the magnet was about 300 Gauss. This was unexpected as the magnet field strength is about an order of magnitude higher than this. This is important to note, because even if a magnet rating is for a specific surface gauss, it may not be what the sensor reads. Additionally, this magnet was placed almost flush to the sensor, which is not realistic for applications. For future testing, perhaps a more powerful magnet is necessary.

IV. CONCLUSION

By the end of this semester, I was able to implement the skills I learned during the first semester to create and implement a 1DOF rig to measure angles using a hall effect sensor. The sensor works by measuring the strength of a magnet in 3 dimensions, and then using trigonometry to determine angles in various planes. The system contained four main components: a mechanical system, encoder and quadrature counter, a motor controller, and a linear hall effect sensor. Additionally, custom libraries for I2C and SPI were used to write source code for the hall effect sensor and encoder. By implementing timers, PI control, and a state machine, the sensor could be tested at various rotations as to compare encoder angles to those captured by the sensor.

A rough relationship between motor rotation and the angle read by the sensor was observed. However, because the original test rig does not have the magnet aligned with the sensor, a new test rig should be developed. This test rig should have the magnet and sensor within the same plane and mounted in a rigid environment. A stronger magnet can also be used. Additionally, averaging techniques should be employed as data is particularly noisy. Long term goals for the project include creating and testing a 2DOF system, integrating the system with wireless units, and designing a PCB/housing unit for the sensor-transmitter pair.

ACKNOWLEDGMENT

Thanks to Bryan Blaise for his guidance throughout the project. He challenged me to figure many concepts on my own, which helped me become a more proficient engineer and coder, and provided valuable assistance when I was stuck. Thanks also to Dr. Hammond for his support for undergraduate research, and for allowing me to work in his lab.

REFERENCES

[1] Cavallari, T. (2013). *Joint Detection Tracking and Mapping (JDTAM) - Computer Vision LAB*. [online] Vision.disi.unibo.it. Available at: http://www.vision.disi.unibo.it/78-cvlab/research/78-cvlab/79-jdtam [Accessed 10 Dec. 2019].

[2] Eisenbeis, R. and Morse, M. (2019). *Overview Using Linear Hall Effect Sensors to Measure Angle*. [online] Available at: http://www.ti.com/lit/an/slya034a/slya034a.pdf [Accessed 10 Dec. 2019].

[3] "Magnetization Direction for Neodymium Magnets," *K&J Magnetics - Magnetization Direction*. [Online]. Available: https://www.kjmagnetics.com/magdir.asp. [Accessed: 01-May-2020].

[4] S. Milne, "On-Axis vs. Off-Axis Angle Sensor IC Measurement Configurations," *Youtube*, 20-Oct-2015. [Online]. Available: https://www.youtube.com/watch?v=BS4MIC-ucq4. [Accessed: 01-May-2020].

[5] Mallon, E. and Beddows, P. (2019). *Tutorial: How to Configure I²C Sensors with Arduino Code*. [online] Underwater Arduino Data Loggers. Available at: https://thecavepearlproject.org/2017/11/03/configuring-i2c-sensors-with-arduino/ [Accessed 10 Dec. 2019].

[6] Allegromicro.com. (2019). *ALS31313: Automotive Grade, 3-D Linear Hall-Effect Sensor*. [online] Available at: https://www.allegromicro.com/en/Products/Sense/Linear-and-Angular-Position/Linear-Position-Sensor-ICs/ALS31313 [Accessed 10 Dec. 2019].

[7] "8995," *DigiKey*. [Online]. Available: https://www.digikey.com/product-detail/en/8995/469-1024-ND/. [Accessed: 01-May-2020].

[8] Sparkfun.com. (2019). *SparkFun Logic Level Converter - Bi-Directional*. [online] Available at: https://www.sparkfun.com/products/12009 [Accessed 10 Dec. 2019].

[9] Pololu.com. (2019). *Pololu - Magnetic Encoder Pair Kit for Micro Metal Gearmotors*. [online] Available at: https://www.pololu.com/product/3081/blog [Accessed 10 Dec. 2019].

[10] USDigital.com. (2019). *LS7366R-S 32-bit Quadrature Counter with Serial Interface*. [online] Available at: https://www.usdigital.com/products/accessories/interfaces/LS7366R-S [Accessed 10 Dec. 2019].

[11] Digikey.com. (2019). *MXO45HS*. [online] Available at: https://www.digikey.com/product-detail/en/cts-frequency-controls/MXO45HS-3C-10M0000/CTX753-ND/1801868 [Accessed 10 Dec. 2019].

[12] Adafruit.com. (2019). *Dual H-Bridge Motor Driver for DC or Steppers*. [online] Available at: https://www.adafruit.com/product/807 [Accessed 10 Dec. 2019].

[13] W. Bussing and R. Bate, "3D Linear or 2D Angle Sensing with the ALS31300 and ALS31313 Hall-Effect ICs," *Allegro Microsystems*. [Online]. Available: https://www.allegromicro.com/en/Insights-and-Innovations/Technical-Documents/Hall-Effect-Sensor-IC-Publications/AN296140-3D-Linear-2D-Angle-Sensing-ALS31300.aspx. [Accessed: 01-May-2020].

[14] R. Hoadley, "A gallery of magnetic fields." [Online]. Available: https://www.coolmagnetman.com/maggallery.htm. [Accessed: 01-May-2020].